



Synthesis of Activated Carbon from Petung Bamboo Stems (*Dendrocalamus Asper*) Using Microwave-Assisted Pyrolysis (MAP) Process for Biogas Storage

Widi Astuti^{1✉}, Triastuti Sulistyaningsih², Raihan Mukti Ramadhan¹, Vista Ayudya Octaviany¹

DOI: <https://doi.org/10.15294/jbat.v11i1.36939>

¹Department of Chemical Engineering, Faculty of Engineering, Universitas Negeri Semarang, Gd. E1 lt.2, Sekaran, Gunungpati, Semarang 50229, Indonesia

²Department of Chemistry, Faculty of Engineering, Universitas Negeri Semarang, Gd. D6 lt.2, Sekaran, Gunungpati, Semarang 50229, Indonesia

Article Info

Article history:

Received

May 2022

Accepted

June 2022

Published

June 2022

Keywords:

Adsorption;

KOH;

Pyrolysis;

Microwave

heating;

Hybrid heating

Abstract

Biogas has emerged as a promising alternative to gasoline due to the depletion of fossil energy and environmental concerns. An investigation was conducted to study the technical feasibility of an adsorbed natural gas (ANG) storage system using petung bamboo-activated carbons. The activated carbons were prepared by microwave-assisted pyrolysis (MAP) and a hybrid heating system for comparison. Microwave-assisted pyrolysis is a promising alternative technology for biochar production because it has several advantages over conventional pyrolysis such as uniform heating temperature, lower energy consumption, and uniform pore size. The characteristics of the obtained activated carbons were evaluated by scanning electron microscope (SEM) and Fourier transform infrared spectroscopy. The results showed that the higher power led to the shorter pyrolysis time. However, at a certain point, the higher power causes the biomass is not degraded completely. In this case, a microwave oven with 2 magnetrons produces a better heating temperature profile than the use of 1 magnetron. The character of activated carbon prepared using 70% power output (1120 W) is better than activated carbon prepared using 60% power output (960 W). In this condition, the pore size is more uniform and the number of functional groups is less. This implies that the petung bamboo activated carbon is the ideal candidate for ANG storage.

INTRODUCTION

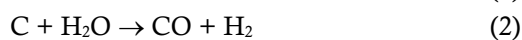
Biogas has emerged as a promising alternative to gasoline due to the depletion of fossil energy and environmental concerns (Li and Su, 2017). Compared to other fuels, biogas containing methane i.e., CH₄ (70-90%) has a clean, safe, and cheap combustion (Sieminsky, 2014) with great efficiency and caloric value, high flammability range, and high auto-ignition temperature (Pratama et al., 2014). However, biogas storage technology is still a serious problem. A storage system using compressed natural gas (CNG) vessel requires very high pressure (20-30 MPa) thus it needs a specially designed pressure vessel with high production and

filling costs (Górniak et al., 2018). The adsorbed natural gas (ANG) storage technique is a promising alternative (Wu et al., 2021). Biogas is adsorbed by a suitable adsorbent (i.e., porous materials) thus higher biogas concentration can be achieved at lower pressure (3.5 MPa) and moderate temperatures (atmospheric conditions). The ANG performance is influenced by adsorbent characters, thermal management during the adsorption process, and vessel design (Khurana et al., 2019). Biogas adsorption on porous materials occurs through van der Waals attraction between biogas (i.e., CH₄) molecules and pore walls, thus the use of suitable adsorbents should be considered to maximize the storage capacity (Zheng et al., 2018).

✉ Corresponding author:
E-mail: widi_astuti@mail.unnes.ac.id

In this case, activated carbon (AC) having a micropore structure and a limited number of functional groups is a promising adsorbent for biogas storage (Mestre et al., 2014) because the existence of functional groups can interfere physiorption process of CH₄ molecules (Kuang et al., 2020).

The most common methods used for AC production are pyrolysis and activation process (Rijali et al., 2015). There are two types of activation processes, namely physical and chemical activation (Zhang et al., 2014). In physical or thermal activation, carbon is modified using two gasifying agents carbon dioxide and water vapor, either singly or together. This agent extracts carbon atoms from the porous carbon structure according to the following reaction (Mistar et al., 2020).



Meanwhile, chemical activation is carried out by immersing biochar in chemicals as activating agents such as phosphoric acid (H₃PO₄), sulfuric acid (H₂SO₄), potassium hydroxide (KOH), sodium hydroxide (NaOH), and zinc chloride (ZnCl₂) (Riyanto et al., 2020). Synthesis of AC derived from mangrove propagule waste using H₃PO₄ as activating agent produced AC with a surface area of 267.45 m²/g (Astuti et al., 2017). Ogungbenro et al., (2020) used palm plants as raw materials with H₂SO₄ activation to produce AC having a surface area of 577.34 m²/g. Coconut shells AC produced through ZnCl₂ activation had a surface area of 15 m²/g (Astuti et al., 2018). Activated carbon derived from ratan plant stalks using NaOH activation had a surface area of 1135 m²/g (Islam et al., 2017), while the use of KOH as an activating agent can produce microporous activated carbon with a high surface area, up to 2000 m²/g (Elmouwahidi et al., 2012; Astuti et al., 2019). Generally, AC produced by chemical activation has advantages including higher yield, larger specific surface area, and better development of porous structure (Mistar et al., 2020). Chemical activation can be carried out in one or two steps. In one step, the activator is mixed with raw materials, while in two steps the activator is mixed with pyrolysis charcoal. In this sense, the microstructure and adsorption characteristics of AC depend on the chemical composition of the raw material, production route (i.e., one or two steps), and conditions of the pyrolysis and activation

process. Therefore, optimization of process conditions is required to synthesize AC for energy and environmental applications.

Several attempts have been made to utilize agricultural residues, forest wastes, and other inexpensive renewable materials as precursors in AC preparation such as rice straw (Chang et al., 2014), tabah bamboo (Negara et al., 2017), tamblang bamboo (Negara et al., 2017), randu wood (Chafidz et al., 2018), coconut shell (Astuti et al., 2018), pineapple leaf (Astuti et al., 2019), petung bamboo (Qanytah et al., 2020), yellow bamboo (Mistar et al., 2020), and corn cobs (Medhat et al., 2021). Petung bamboo stem waste contains 45.02% cellulose, 10.81% hemicellulose, and 28.35% lignin with a low inorganic content (Larasati et al., 2019) which can be used as raw materials in the AC preparation (Krismayanti et al., 2018).

Utilization of petung bamboo stem waste as raw material in the AC preparation has been carried out by Qanytah et al., (2020). The AC obtained has a pore diameter of 1.18 nm which belongs to the micropore type. Another study that also used petung bamboo as a precursor in the AC preparation showed a surface area of 1954.95 m²/g (Wirawan et al., 2018). Both studies used conventional heating, i.e., furnace. In conventional heating, energy is transferred from a heat source located outside the material bed to the interior through convection, conduction, and radiation mechanism. It produces a thermal gradient in the material from the hottest surface to the interior until steady conditions are reached. To solve the thermal gradient problem, a slower heating rate is used. It results in a longer heating time and increased energy consumption. The existence of a temperature gradient causes the pores of the activated carbon to be non-uniform (Ahmed, 2016). Nowadays, microwave heating is a viable alternative to conventional heating. Unlike conventional heating, microwave heating is internal and volumetric in that there is no temperature gradient in the material bed, resulting in biochar with a more uniform pore size (Ao et al., 2018). This research used a microwave oven with 2 magnetrons to produce a more even heat distribution. In this sense, the effect of power on the temperature profile as well as the yield and character of petung bamboo stems AC are discussed further.

MATERIALS AND METHODS

Materials

The petung bamboo used as a precursor in this study was obtained from Magelang, Indonesia. Potassium hydroxide (KOH) and hydrochloric acid (HCl) were acquired from Merck (Germany).

Preparation of Petung Bamboo Powder

The petung bamboo powder was dried in sunlight for one day, then sieved using a 10-18 mesh sieve and heated using an oven (Memmert type UN55, Germany) at a temperature of 105°C until the dried sample weight was constant.

Preparation of Activated Carbon

Microwave-assisted pyrolysis of bamboo powder was carried out by loading 50 g of dry sample into an alumina reactor installed in a microwave oven (Electrolux type EMM 2308 with modification of 2 magnetrons). Pyrolysis was carried out under a stream of N₂ with a flow rate of 100 cm³/min at 60% (960W) and 70% (1120W) power output while the final temperature was set at 500°C. After cooling to ambient temperature, the obtained biochar was weighed. The yield of biochar was calculated using Eq. (3).

$$\text{yield of biochar (\%)} = \frac{\text{weight of biochar}}{\text{weight of bamboo powder}} \times 100\% \quad (3)$$

The biochar was further mixed with KOH and 10 mL of distilled water, and stirred for 120 minutes. The weight ratio of KOH: biochar was 3:1. Biochar was then dried using an oven at 105°C for 24 hours before activation process. In the activation process, the impregnated biochar was placed in an alumina reactor installed in the microwave oven (Electrolux type EMM 2308 with modification of 2 magnetrons). The activation process was conducted at a power output of 70% (1120W) under a nitrogen flow rate of 100 cm³/min until the temperature reach 500°C (Astuti et al., 2019). The activated carbon was washed using 0.1 M HCl and distilled water until the pH reached 6.5-7. In the last stage, the activated carbon was dried using an oven at 110°C for 24 hours (Mistar et al., 2020).

Characterization of Adsorbent

The surface morphology of the biochar and activated carbon were analyzed using Scanning Electron Microscope with Energy Dispersive X-ray

(SEM-EDX) (JSM-6360). The surface functional groups of the biochar and activated carbon were analyzed using Fourier Transform Infrared (FTIR) Spectroscopy (Perkin Elmer Spectrum IR 10.6.1) recorded between 450 and 4000 cm⁻¹.

RESULTS AND DISCUSSION

Effect of Microwave Power on The Pyrolysis Temperature Profile

The use of microwaves in the pyrolysis process can improve the properties and character of biochar. In this sense, microwave power is an important factor because it can affect the heating rate. Higher power can increase the interaction between the material and the microwave field leading to rotation, collision, torsion, and friction of the molecules in the material thereby increasing the potential to convert absorbed microwaves into thermal energy. On the other hand, if the microwave power is too low, the interaction between the material and the microwave is too weak and causes molecular cleavage (Y. Zhang et al., 2022). The temperature profile at various microwave power is presented in Figure 1. Based on Figure 1, it can be seen that the temperature profile for each microwave is different. At a power output of 50% (800 W), the temperature increase was very slow and can only reach the final temperature of 242°C, far from the desired pyrolysis temperature (500°C). It takes 34 minutes to reach temperature of 240°C, after 34 minutes temperature dropped slightly and then constant at 235°C. Meanwhile, at 80% power output (1280 W) the temperature rise too fast in which the temperature of 500°C was reached in just 2 minutes. The higher the microwave power used, the greater the amount of microwave energy received by the biomass so that the temperature increase very fast and the time required to reach the desired pyrolysis temperature (500°C) is also shorter. At the power usage of 960 W and 1120 W, the temperature profile is declivous compared to the power usage of 1280 W where the temperature of 480°C was reached in 10 and 8 minutes, respectively.

Referring to the fact that pyrolysis temperature profile can greatly affect the morphological structure of the biochar produced, this study also carried out a micro-hybrid heating system (Figure 2) as a comparison. In the micro-hybrid system (Figure 3), the temperature rise is unstable, especially at low power and it requires

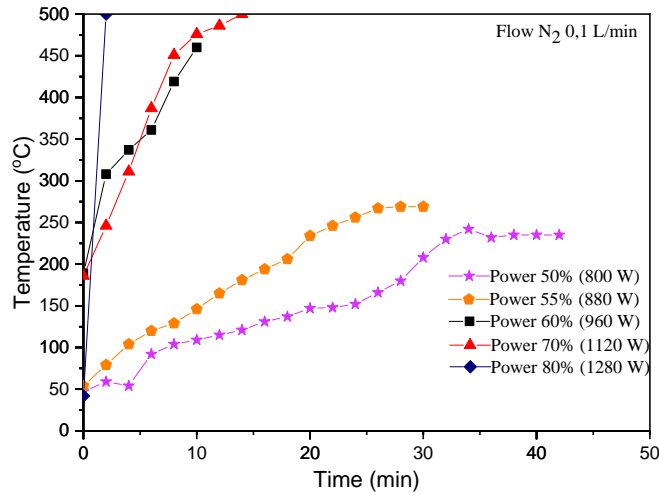


Figure 1. Temperature Profile at Various Microwave Powers.

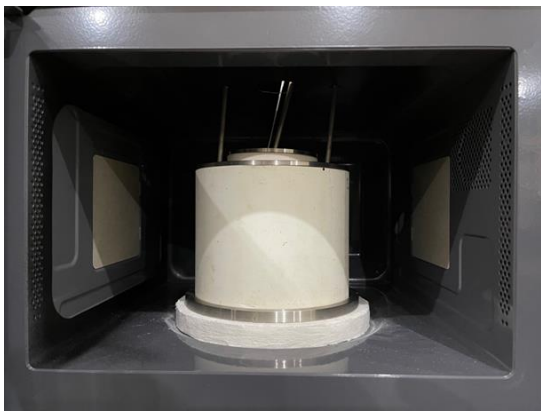


Figure 2. Alumina Reactors for Micro-Hybrid Heating System. (Larger reactor containing coconut shell charcoal, smaller reactor containing biomass sample).

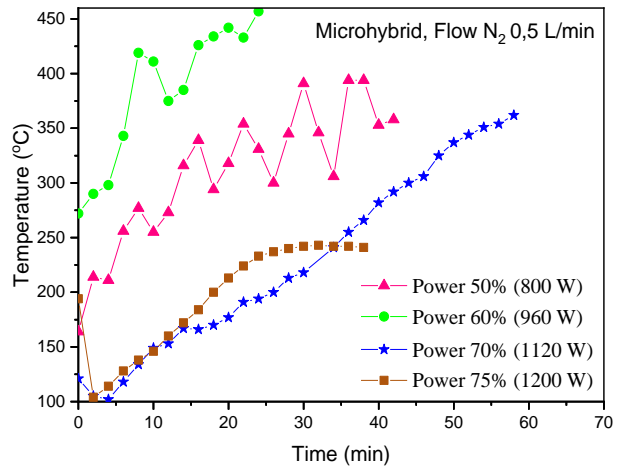


Figure 3. Temperature Profile at Various Power for Microhybrid System.

longer time than microwave heating. In addition, the desired final pyrolysis temperature (500°C) cannot be achieved at all the power used, in which the highest temperature is only 450°C at 60% output power (i.e., 960 W). Temperature instability in the micro-hybrid system may be due to the presence of two heating mechanisms that occur simultaneously but both have different time intervals. Some microwave radiation is absorbed by coconut shell charcoal, converted to heat, and then transmitted to the biomass by a conduction mechanism through reactor walls. While some other microwave radiation can be directly absorbed by the biomass and converted to heat. Therefore, at low power usage (50 and 60%), the temperature instability is very obvious because the low heating rate causes the conduction process slower. The temperature instability diminished with higher power usage, but

the achievable temperature is lower. As a result, the biomass degradation process is incomplete, as shown in Figure 4(h)-(i). At 960W, the maximum achievable temperature is 450°C. As is known, biomass composed of hemicellulose, cellulose, and lignin is degraded at temperatures of 220-300°C, 300-340°C, and 300-900°C, respectively. Therefore, at 450°C all the biomass should have been degraded. The imperfection of the pyrolysis process at a temperature of 450°C (Figure 4.3(f)) may be caused by temperature instability. Therefore the temperature profile is a very important parameter to consider in the pyrolysis process. Meanwhile, Figure 4(e) shows that biomass degradation has not occurred yet. This is probably due to the very short pyrolysis time (<2 minutes) even though the pyrolysis temperature of 500°C has been reached.

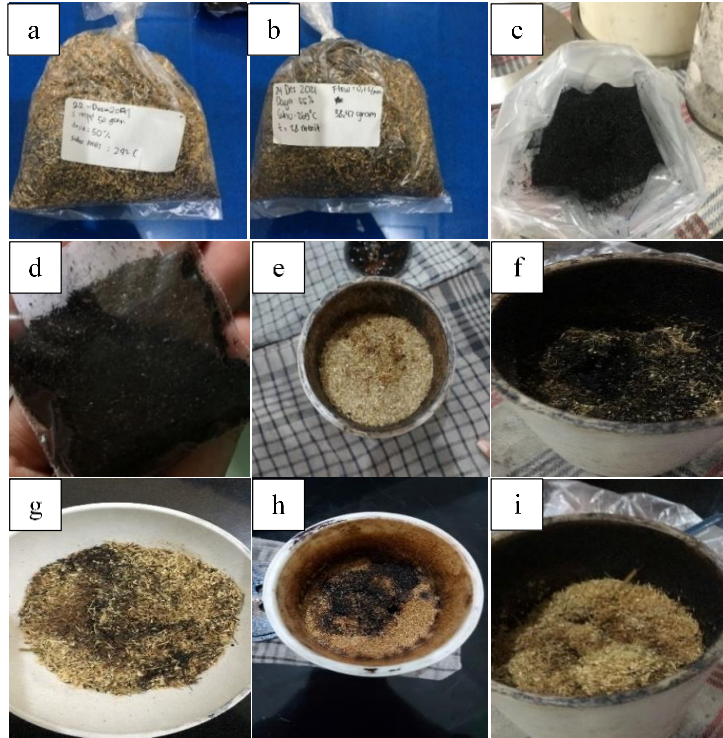


Figure 4. Pyrolysis Results at a certain Power (a) microwave, 50% power output (800 W); (b) microwave, 55% power output (880 W); (c) microwave, 60% power output (960 W); (d) microwave, 70% power output (1120 W); (e) microwave, 80% power output (1280 W); (f) micro-hybrid, 50% power output (800 W); (g) micro-hybrid, 60% power output (960 W); (h) micro-hybrid, 70% power output (1120 W); (i) micro-hybrid, 75% output (1200 W).

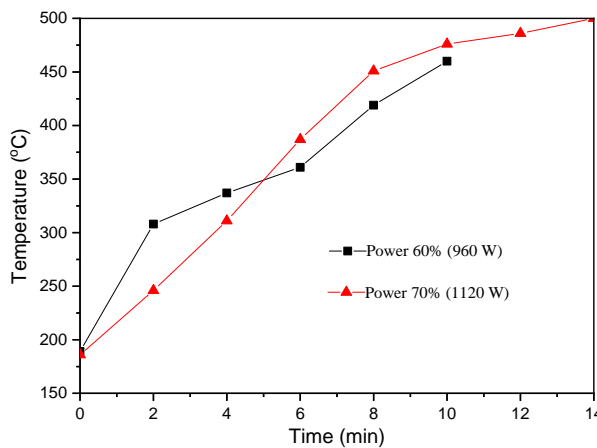


Figure 5. Temperature Profiles at 960W and 1120W.

Bamboo stem powder can be completely degraded using a microwave heating system with 60% output power (960 W) and 70% output power (1120 W), as shown in Figures 4(c) and (d). Under these conditions, the temperature rise is stable and the final temperature reaches 500°C (Figure 5).

Therefore, this study only focuses on the power usage of 960W and 1120W.

Effect of Microwave Power on The Biochar Yield

Figure 6 shows that increasing microwave power decreases biochar yield due to the intensified interaction between biomass and microwave (Lam et al., 2017). After the degradation process of bamboo powder is complete, further heating causes some carbon atoms in biochar react with CO₂ and H₂O resulting from pyrolysis, according to reactions (4) and (5), thereby reducing the yield of biochar. The increase in power from 960 W to 1120 W reduced the yield by 1.24% (from 35.32 to 34.08%).



Although yield of biochar produced at 1120 W (namely B1120) is lower than yield of biochar produced at 960 W (namely B960), the purity of

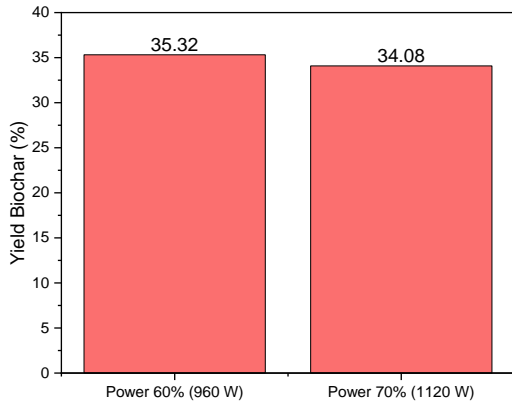
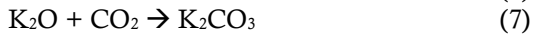
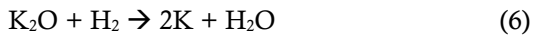


Figure 6. Graph of Effect of Microwave with Yield Biochar Pyrolysis Results.

B1120 is higher (carbon content of 82.98%) than B960 (carbon content of 72.22%). It may be due to some impurities such as K_2O being lost on high-intensity heating thereby the carbon content increases. K_2O can react with H_2 , CO_2 , and C according to Eq. (6)-(8). As a result, K_2O content in B960 is higher (14.33%) than in B1120 (7.89%).



Effect of Microwave Power on The Biochar and Activated Carbon Morphology

As previously explained, further heating after the biomass degradation process is completed

causes some carbon atoms react with CO_2 and H_2O to CO gas. The partial cleavage of the C bonds due to this reaction causes an increase in the pore size of the biochar. Therefore, the higher microwave power used, the larger pore size, as shown in Figures 7(a) and (c). In addition, B1120 in Figure 7(c) has a more uniform pore size than B960 in Figure 7(a). It may be due to the stability of temperature rise, as shown in Figure 5. Significant changes in the surface morphology of biochar are clearly seen after the activation process with KOH , especially at B960. The pores become very large, much larger than the pores of B1120 after activation process. The development of porosity by KOH follows the following reaction.



Diffusion of potassium (K) compounds into biochar widens the existing pores because these compounds can function as templates in the formation of pores. In addition, reaction (10) also contributes to the formation of new pores. As previously explained, B960 contains more K_2O from biomass impurities, in which K_2O also contributes to the activation process according to Eq. (10). Therefore, activated carbon resulting from activation of B960 (namely AC960) has a larger pore size than that of B1120 (namely AC1120). As previously explained, the

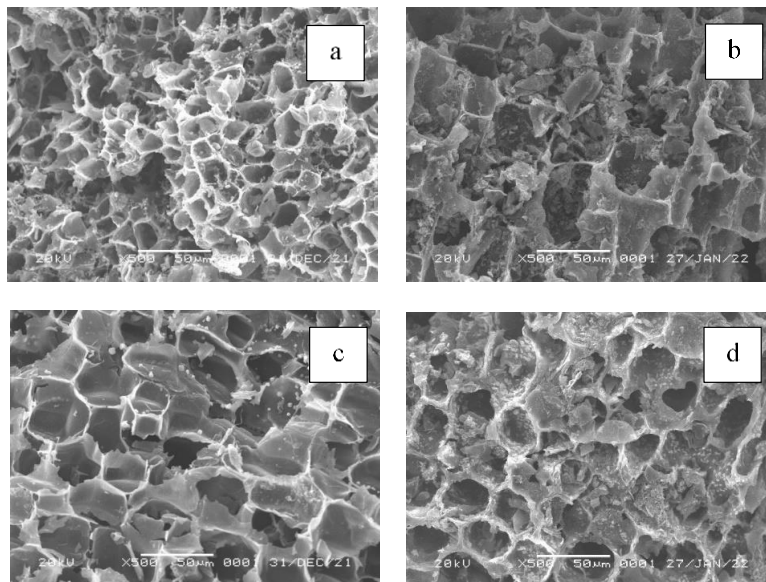


Figure 7. Morphology of (a) Biochar at 60% power output (B960), (b) Activated Carbon at 60% power output (AC960), (c) Biochar at 70% power output (B1120), (d) Activated Carbon at 70% power output (AC1120) (Magnification: 500x).

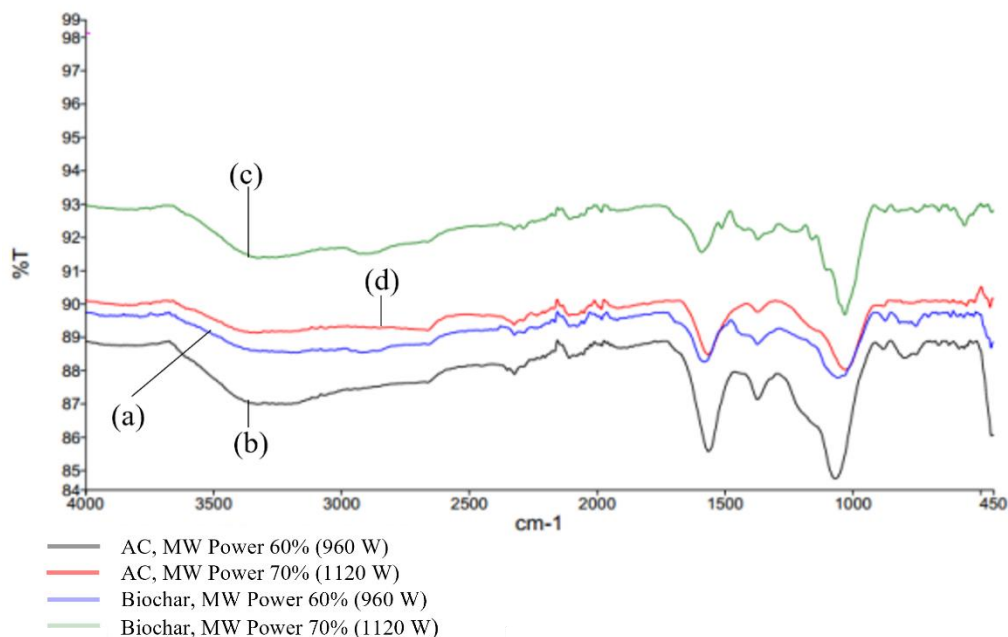


Figure 8. FTIR Spectrum on (a) Biochar (b) 60% Power Activated Carbon (c) Biochar (d) 70% Power Activated Carbon.

activation process according to Eq. (10) causes a partial loss of C, thereby the C content after the activation process decreased from 72.22% to 66.35% for AC960 and from 82.93% to 67.83% for AC1120. Figure 6 also shows that AC960 is more brittle than AC1120. AC960 pore walls are thinner and some pores are destroyed. It is because the higher power leads to an increase in carbon content and a decrease in O and H content, or in other words the H/C ratio decreases. The smaller H/C ratio leads to a higher aromatization and a more stable biochar structure, as shown in AC1120 (X. Zhang et al., 2022).

Effect of Microwave Power on The Surface Functional Groups

To confirm the presence of surface functional groups in biochars and ACs, FTIR analysis was conducted. Figure 8(a) shows biochar B960 has an absorption peak at 3198.53 cm⁻¹ indicating the presence of a hydroxyl (O-H) group (Saad et al., 2019). The peak at 1373.22 cm⁻¹ is assigned to the aliphatic deformation of CH₂ or CH₃ groups or O-H bending of phenolic. The existence of an absorption peak around 1580.14 cm⁻¹ is attributed to the C=C stretching vibrations of aromatic compounds (Astuti et al., 2018), while a peak observed at 1059.18 cm⁻¹ may be attributed to the C-O group (Saafie et al., 2019). After the activation process with KOH (Figure 8(b)), the peak of B960 at 1373.22 cm⁻¹ shifts to 1372.86 cm⁻¹,

indicating aromatization and dehydration occurred as a result of the decomposition and condensation of volatile matters (Saad et al., 2019). Meanwhile, the band at 3198.53 cm⁻¹ for OH stretching deepens and shifts to 3330.28 cm⁻¹. It is due to ion exchange between K⁺ on -OK group and H⁺ on H₂O during the washing process, forming the -OH functional group (Oginni et al., 2019; Saad et al., 2019). Meanwhile, the C=C group as indicated by an absorption peak at 1580.14 cm⁻¹ shifts to 1564.89 cm⁻¹ and deepens. It may be due to the decomposition of the C-H bond to produce aromatic C=C bonds which is more stable at high temperatures (Saad et al., 2019).

Figure 8(c) shows that biochar B1120 has an absorption peak at 3330.99 cm⁻¹ indicating the presence of a hydroxyl group (O-H) (Saad et al., 2019). The peak observed around 1591.23 cm⁻¹ may be attributed to the C=C stretching vibration of aromatic compounds (Astuti et al., 2018), while the band at 1030.69 cm⁻¹ reflects C-O group (Saad et al., 2019). After activation with KOH (Figure 8(d)), the absorption peak at 3300-3700 cm⁻¹ indicates the existence of the -OH group is shallower. It is in contrast to biochar B960 which is deeper after the activation process. The decrease in the number of -OH groups in AC1120 may be due to the larger pore size of B1120, thereby more -OH groups can be released as H₂O during the activation process. Meanwhile, the C=C group indicated by an absorption peak at 1591.23 cm⁻¹ shifts to 1564.89

cm⁻¹ and deepens. It may be due to the decomposition of the C-H bond to produce aromatic C=C bonds which is more stable at high temperatures (Saad et al., 2019) and create new pores (Astuti et al., 2018).

Based on the FTIR results, it can be seen that AC1120 is better than AC960 because it contains fewer functional groups. As is known, the higher number of functional groups leads to the gas physisorption process is disturbed (Kuang et al., 2020).

CONCLUSION

The higher power used in microwave-assisted pyrolysis (MAP) leads to a more stable heating temperature profile indicated by no significant increase or decrease in temperature. In the power range studied (power output of 60 and 70%), a greater power used leads to a lower biochar yield. The character of activated carbon produced using 70% power output (AC1120) is better than activated carbon produced using 60% power output (AC960), i.e., better surface morphology and fewer functional groups.

REFERENCES

- Ahmed, M. J. 2016. Application of agricultural based activated carbons by microwave and conventional activations for basic dye adsorption: Review. *Journal of Environmental Chemical Engineering*. 4(1): 89–99.
- Ao, W., Fu, J., Mao, X., Kang, Q., Ran, C., Liu, Y., Zhang, H., Gao, Z., Li, J., Liu, G., Dai, J. 2018. Microwave assisted preparation of activated carbon from biomass: A review. *Renewable and Sustainable Energy Reviews*. 92(July 2017): 958–979.
- Astuti, W., Dwi Handayani, A., Wulandari, D. A. 2018. Adsorpsi Methyl Violet oleh Karbon Aktif dari Limbah Tempurung Kelapa dengan Aktivator ZnCl₂ Menggunakan Pemanasan Gelombang Mikro. *Jurnal Rekayasa Kimia & Lingkungan*. 13(2): 189–199.
- Astuti, W., Hermawan, R. A., Mukti, H., Sugiyono, N. R. 2017. Preparation of activated carbon from mangrove propagule waste by H₃PO₄ activation for Pb²⁺ adsorption. *AIP Conference Proceedings*. 1788: 1–6.
- Astuti, W., Sulistyaningsih, T., Kusumastuti, E., Thomas, G. Y. R. S., Kusnadi, R. Y. 2019. Thermal conversion of pineapple crown leaf waste to magnetized activated carbon for dye removal. *Bioresource Technology*. 287(April). 121426.
- Chafidz, A., Astuti, W., Augustia, V., Novira, D. T., Rofiah, N. 2018. Removal of methyl violet dye via adsorption using activated carbon prepared from Randu sawdust (*Ceiba pentandra*). *IOP Conference Series: Earth and Environmental Science*. 167(1).
- Chang, K. L., Chen, C. C., Lin, J. H., Hsien, J. F., Wang, Y., Zhao, F., Shih, Y. H., Xing, Z. J., Chen, S. T. 2014. Rice straw-derived activated carbons for the removal of carbofuran from an aqueous solution. *Xinxing Tan Cailiao/New Carbon Materials*. 29(1): 47–54.
- Coates, J. 2019. Interpretation of Infrared Spectra, A Practical Approach. *Encyclopedia of Analytical Chemistry*. 1–23.
- Elmouwahidi, A., Zapata-Benabithé, Z., Carrasco-Marín, F., Moreno-Castilla, C. 2012. Activated carbons from KOH-activation of argan (*Argania spinosa*) seed shells as supercapacitor electrodes. *Bioresource Technology*. 111: 185–190.
- Górniak, A., Midor, K., Kaźmierczak, J., Kaniak, W. 2018. Advantages and Disadvantages of Using Methane from CNG in Motor Vehicles in Polish Conditions. *Multidisciplinary Aspects of Production Engineering*. 1(1): 241–247.
- Islam, M. A., Ahmed, M. J., Khanday, W. A., Asif, M., Hameed, B. H. 2017. Mesoporous activated carbon prepared from NaOH activation of rattan (*Lacosperma secundiflorum*) hydrochar for methylene blue removal. *Ecotoxicology and Environmental Safety*. 138(August 2016): 279–285.
- Jiang, Y., Zong, P., Tian, B., Xu, F., Tian, Y., Qiao, Y., Zhang, J. 2019. Pyrolysis behaviors and product distribution of Shenmu coal at high heating rate: A study using TG-FTIR and Py-GC/MS. *Energy Conversion and Management*. 179(October 2018): 72–80.

- Khurana, M., Veluswamy, H. P., Daraboina, N., Linga, P. 2019. Thermodynamic and kinetic modelling of mixed CH₄-THF hydrate for methane storage application. *Chemical Engineering Journal*. 370(January): 760–771.
- Krismayanti, N. P. A., Manurung, M., Suastuti, N. G. A. M. D. A. 2018. Sintesis Arang Aktif Dari Limbah Batang Bambu Dengan Aktivator Naoh Sebagai Adsorben Ion Krom (Iii) & Timbal (Ii). *Cakra Kimia*. 7(Iii): 189–197.
- Kuang, Y., Zhang, X., Zhou, S. 2020. Adsorption of methylene blue in water onto activated carbon by surfactant modification. *Water (Switzerland)*. 12(2): 1–19.
- Lam, S. S., Liew, R. K., Wong, Y. M., Azwar, E., Jusoh, A., Wahi, R. 2017. Activated Carbon for Catalyst Support from Microwave Pyrolysis of Orange Peel. *Waste and Biomass Valorization*. 8(6): 2109–2119.
- Larasati, I. A., Argo, D., Hawa, L. C., Keteknikan, J., Teknologi, P.-F., Brawijaya, P.-U., Veteran, J., Korespondensi, P. 2019. Proses Delignifikasi Kandungan Lignoselulosa Serbuk Bambu Betung dengan Variasi NaOH & Tekanan. *Jurnal Keteknikan Pertanian Tropis & Biosistem*. 7(3): 235–244.
- Li, R., Su, M. 2017. The role of natural gas and renewable energy in curbing carbon emission: Case study of the United States. *Sustainability (Switzerland)*. 9(4): 18–20.
- Medhat, A., El-Maghrabi, H. H., Abdelghany, A., Abdel Menem, N. M., Raynaud, P., Moustafa, Y. M., Elsayed, M. A., Nada, A. A. 2021. Efficiently activated carbons from corn cob for methylene blue adsorption. *Applied Surface Science Advances*. 3(November 2020): 100037.
- Mistar, E. M., Alfatah, T., Supar, M. D. 2020. Synthesis and characterization of activated carbon from *Bambusa vulgaris striata* using two-step KOH activation. *Journal of Materials Research and Technology*. 9(3): 6278–6286.
- Oginni, O., Singh, K., Oporto, G., Dawson-Andoh, B., McDonald, L., Sabolsky, E. 2019. Influence of One-step and Two-step KOH Activation on Activated Carbon Characteristics. *Bioresource Technology Reports*. 7: 100266.
- Ogunbenro, A. E., Quang, D. V., Al-Ali, K. A., Vega, L. F., Abu-Zahra, M. R. M. 2020. Synthesis and characterization of activated carbon from biomass date seeds for carbon dioxide adsorption. *Journal of Environmental Chemical Engineering*. 8(5): 104257.
- Pratama, I., Martin, A., Nasruddin. 2014. Adsorption Isothermal Methane Gas With Mass Flow Rate of 10 SLP Mand 20 SLP For Adsorbed Natural Gas Storage. 3(57): 29–39.
- Negara, D. N. K. P, Tirta Nindhia, T. G., Surata, I. W., Sucipta, M. 2017. Chemical, strength and microstructure characterization of Balinese bamboos as activated carbon source for adsorbed natural gas application. *IOP Conference Series: Materials Science and Engineering*, 201(1): 012033.
- Qanytah, Syamsu, K., Fahma, F., Pari, G. 2020. Characterization of Ball-Milled Bamboo-Based Activated. *Peer-Reviewed Article*. 15: 8303–8322.
- Rijali, A., Malik, U., Zulkarnain. 2015. Pembuatan & Karakterisasi Karbon Aktif dari Bambu Betung dengan Aktivasi Menggunakan Activating Agent H₂O. *JOM FMIPA*. 148(1): 148–162.
- Riyanto, C. A., Ampri, M. S., Martono, Y. 2020. Synthesis and Characterization of Nano Activated Carbon from Annatto Peels (*Bixa orellana* L.) Viewed from Temperature Activation and Impregnation Ratio of H₃PO₄. *EKSAKTA: Journal of Sciences and Data Analysis*. 1(1): 44–50.
- Rodrigues Teixeira, A. C., Machado, P. G., Borges, R. R., Felipe Brito, T. L., Moutinho dos Santos, E., Mouette, D. 2021. The use of liquefied natural gas as an alternative fuel in freight transport – Evidence from a driver’s point of view. *Energy Policy*. 149(December): 112106.
- S. Mestre, A., Freire, C., Pires, J., P. Carvalho, A., L. Pinto, M. 2014. High performance microspherical activated carbons for methane storage and landfill gas or biogas upgrade. *Journal of Materials Chemistry*. 1–30.

- Saad, M. J., Chia, C. H., Zakaria, S., Sajab, M. S., Misran, S., Rahman, M. H. A., Chin, S. X. 2019. Physical and chemical properties of the rice straw activated carbon produced from carbonization and KOH activation processes. *Sains Malaysiana*. 48(2): 385–391.
- Saafie, N., Samsudin, M. F. R., Sufian, S., Ramli, R. M. 2019. Enhancement of the activated carbon over methylene blue removal efficiency via alkali-acid treatment. *AIP Conference Proceedings*. 2124(July).
- Sieminsky, A. 2014. *International Energy Outlook*. Outlook. November: 70–99.
- Veluswamy, H. P., Kumar, A., Seo, Y., Lee, J. D., Linga, P. 2018. A review of solidified natural gas (SNG) technology for gas storage via clathrate hydrates. *Applied Energy*. 216(September 2017): 262–285.
- Wirawan, I. P. S., Sutrisno, S., Seminar, K. B., Nelwan, L. O. 2018. Characteristics of Microactive Carbon from Bamboo Var. *Petung as Adsorbent*. IOP Conference Series: Earth and Environmental Science. 147(1).
- Wu, Z., Wee, V., Ma, X., Zhao, D. 2021. Adsorbed Natural Gas Storage for Onboard Applications. *Advanced Sustainable Systems*. 5(4): 1–16.
- Yang, K., Zhang, Y., Dong, Y., Peng, J., Kaal, J., Li, W., Ma, X., Nie, Z. 2021. Tracking variations in the abundance and composition of dissolved organic matter in solar ponds of oilfield-produced brine. *Applied Geochemistry*. 131(March): 105008.
- Zhang, X., Zhao, B., Liu, H., Zhao, Y., Li, L. 2022. Effects of pyrolysis temperature on biochar's characteristics and speciation and environmental risks of heavy metals in sewage sludge biochars. *Environmental Technology and Innovation*. 26: 102288.
- Zhang, Y., Fan, S., Liu, T., Fu, W., Li, B. 2022. A review of biochar prepared by microwave-assisted pyrolysis of organic wastes. *Sustainable Energy Technologies and Assessments*. 50: 101873.
- Zhang, Y. J., Xing, Z. J., Duan, Z. K., Li, M., Wang, Y. 2014. Effects of steam activation on the pore structure and surface chemistry of activated carbon derived from bamboo waste. *Applied Surface Science*. 315(1): 279–286.
- Zheng, Y., Li, Q., Yuan, C., Tao, Q., Zhao, Y., Zhang, G., Liu, J., Qi, G. 2018. Thermodynamic analysis of high-pressure methane adsorption on coal-based activated carbon. *Fuel*. 230(May): 172–184.